Iranian Journal of Science and Technology, Transactions of Mechanical Engineering
https://doi.org/10.1007/s40997-022-00559-0

RESEARCH PAPER

Experimental Investigations of a Minichannel Heat Sink for Electronic Applications

Kamlesh Mehta[1] · **Vivek Patel**[2,3] · **Nirvesh Mehta**[4] · **Amarish Badgujur**[5]

Received: 29 April 2022 / Accepted: 8 November 2022
© The Author(s), under exclusive licence to Shiraz University 2022

Abstract

In the current study, a new configuration of minichannels is proposed to improve the thermal performance of conventional plate-fin aluminum heat sink used for the thermal management of the electronic components. The case under consideration to implement the current idea is an aluminum heat sink equipped with rectangular square minichannels. Hence, an enhanced model is investigated, and the obtained results are evaluated as compared with the conventional plate-fin aluminum heat sink. A minichannel heat sink (MC-HS) that has 18 parallel minichannels was developed on the aluminum plate and charged with acetone. The experimental results demonstrated that the proposed MC-HS startup was successfully under a heat load ranging from 10 to 40 W in the vertical orientation. From the investigations, a MC-HS is found to be more effective for the thermal management of the electronic components than the conventional method. The thermal resistance of the MC-HS is 20–31% lower in comparison with the conventional plate-fin aluminum heat sink. It is shown that the MC-HS not only surpasses the conventional solution but also provides greater thermal management of the electronic components.

Keywords Experimental evaluation · Heat sink · Heat dissipation · Oscillatory motion

Abbreviations

Bo	Bond number, $\frac{g(\rho l-\rho v)r_h}{\sigma}^2$
g	Gravitational force, m/s^2
ρ_l	Liquid density, kg/m^3
ρ_v	Vapor density, kg/m^3
r_h	Hydraulic radius, mm
σ	Surface tension, N/m
Q	Heat load, W
R_{th}	Thermal Resistance, °C/W
U	Internal energy, J
T	Temperature, °C

Subscripts

CLFP-OHP	Closed-loop flat plate oscillating heat pipe
FP-OHP	Flat plate oscillating heat pipe
MC-HS	Minichannel heat sink
E	Evaporator
C	Condenser
L	Liquid
V	Vapor
W	Watt

✉ Kamlesh Mehta
kameshnit1@yahoo.com

Vivek Patel
profvvp@yahoo.com; vivek.patel@hv.se

Nirvesh Mehta
vpmpmechanical@gmail.com

Amarish Badgujur
amarishb@nuv.ac.in

[1] Department of Mechanical Engineering, Gujarat Technological University, Ahmedabad, Gujarat 382424, India

[2] Division of Welding Technology, University West, 46186 Trollhattan, Sweden

[3] Northwestern Polytechnical University, Shaanxi, China

[4] Department of Mechanical Engineering, Government Engineering College, Dahod, Gujarat 389151, India

[5] Department of Mechanical Engineering, Navrachna University, Vadodara, Gujarat, India

1 Introduction

Heat sinks have been incorporated into the thermal management of electronic systems (Hosseinirad et al. 2019). Generally, these conventional heat sinks are designed and manufactured in different shapes (Chamanroy and Khoshvaght-Aliabadi 2019; Gholinia et al. 2022a, 2021, 2022b). With the rapid development of the electronic industry, the heat flux in electronic components has almost reached its

Published online: 22 November 2022

limit at about 100 W/cm^2 (Xie et al. 2007). Therefore, the research for more efficient heat sink technologies becomes essential for the further development of the electronic industry. The increasing miniaturization of electronic systems and their components is setting more demanding criteria regarding the thermal management of electronic systems. A common thermal management technique for many electronic components is to use either free convection or forced convection. With the development of technology, electronic components such as IGBTs, Mosfets, and Diodes have been widely used in the field of electronics industries. The ITRS (International Technology Roadmap for semiconductors) predicts that by 2022 the average power consumption for the electronics component to be over 400 W and over 800 W by 2026 (Liang et al. 2019). As a result of the miniaturization within a small area, together with the power required to operate these electronics component, the quantity of heat generated by components has increased. This heat must be dissipated to maintain the electronic components at an acceptable operating temperature range. The conventional cooling solutions such as the plate-fin aluminum heat sink, and air have now effectively reached their limits (Sun et al. 2021; Lu et al. 2021; Bedi and Subbarao 2021; Sivasankaran and Narrein 2020; Taghilou et al. 2022). Published studies on conventional heat sinks are reviewed here. Hashemi et al. (Hashemi et al. 2012) numerically studied the heat transfer and flow in a plate-fin heat sink. The effects of channel were investigated. It was found that the use of minichannel in plate-fin heat sink can increase the heat transfer performance. Arshad et al. (Arshad and Ali 2017) experimentally investigated the heat transfer and effect of water/graphene nanofluid inside the plate-fin heat sink. It was observed higher values of heat transfer. Liu et al. (Bao-Min 2004) numerically proposed a microprocessor package with a narrow water jacket to cool a thermal spread attached to the electronic component. The minichannel flow geometry offers a large surface area of heat transfer and a high convective heat transfer (Xie et al. 2007). Ghasemi et al. evaluated the effect of Al_2O_3 nanoparticles in a minichannel heat sink for heat dissipation from central processing unit (Ghasemi et al. 2021). To improve the thermal performance of liquid-cooled heat sinks, the use of nanofluid has been considered (Ghasemi et al. 2017a). TiO_2 nanofluids to increase the heat transfer in the minichannel heat sinks were investigated by Ghasemi et al. (Ghasemi et al. 2017b). Therefore, Fluid flow in a minichannel and convective heat transfer and their application in the cooling technology of electronic components has attracted the great attention of researchers in recent years (Ghasemi et al. 2017c, 2017d, 2017e, 2017f, 2018). It is worth noting that the lack of sufficient research on the using minichannel charged with acetone in heat sink modules is quite obvious, therefore, this article intends to fill this gap using the experimental investigations.

1.1 Concept of Minichannel Heat Sink

The heat sink material has higher thermal resistance or low thermal conductance, which impedes the electronic component heat transfer rate. The plate-fin aluminum heat sink can improve the cooling capacity by increasing the surface area of the cooling fins, but it is constrained by the space for installation (Wang et al. 2017; Marcinichen et al. 2013; Mudawar 2013; Li et al. 2021). Therefore, if heat generation by electronics components is to increase further in the coming years, more effective cooling methods will be needed. A new heat transfer device must effectively transfer the heat from the electronic components. The systematic dissipation of heat from the constrained areas of microelectronic components makes thermal management to be a challenging job and needs a more cost-effective and reliable solution (Gnanadurai and Varadarajan 2016; Mehta and Mehta 2016; Kavoosi Balotaki and Saidi 2019; Mohsen et al. 2021). One method for reduction in thermal resistance and increasing the thermal conductivity of the heat sink is to incorporate two phase heat transfer, and this is accomplished by the minichannel in the heat sink by experimentally characterizing its thermal performance while it is bottom heated and uniformly cooled with flowing air. The MC-HS is a relatively new type of two phase heat transfer device. The MC-HS is of a more simple structure and has some additional advantages like miniaturization, high heat transfer capacity, flexibility, and low cost over the traditional heat pipe (Liu et al. 2019; Al-Zaidi et al. 2018; Mehta et al. 2020a, 2020b; Qi et al. 2020; He et al. 2020; Fairley et al. 2015). The MC-HS consists of parallel minichannels machined in a metal plate as shown in Fig. 1.

The idea of the minichannel on metal plates has been substantially investigated as an oscillating heat pipe (OHP) in the past few years due to its high heat transfer potential and its viable candidacy for various thermal management solutions. In contrast to the traditional heat pipe, the OHP has lower resistance with no wicking structure, and exists

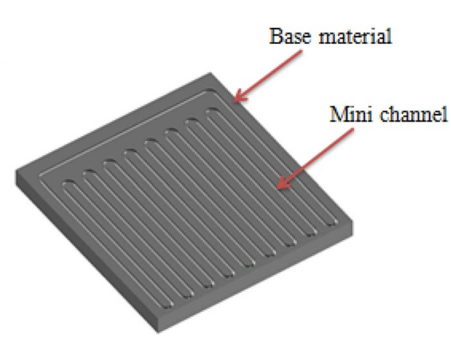

Fig. 1 Concept of minichannel on metal plate (Mehta et al. 2020a, 2020c; Cheng et al. 2010)

as a flat shape (Zhang et al. 2021). The MC-HS embedded with OHP is partially charged with a working fluid and the hydraulic radius of the channel is made sufficiently small in order to form stable liquid slugs and vapor plugs to form two phase heat transfer. The MC-HS device structure is designed to meander through an evaporator section and condenser section multiple times so that, during operation, the continuous liquid slugs and vapor plugs create an unbalance, nonuniform vapor pressure that displaces liquid slugs and vapor plugs to and from the evaporator section in an oscillatory motion (Ayel et al. 2018). This results in a cyclic two phase heat transfer process consisting of both latent heat and sensible heat transfer. In order to understand the MC-HS more clearly, the experimental data of previous research are summarized in Table 1. Previous researchers have investigated the thermal performance of CLFP-OHPs with operational and geometrical parameters. Till date there is no best model of thermal management for electronic applications which can give the optimum thermal performance over a wide range of operations. As a result, the OHP has not been extensively used for electronic systems. The MC-HS has a geometrical advantage for miniaturization and direct integration in electronic components because of its relatively simple structural design. However, results and discussions of the previous investigations have characterized the OHP only for axial heating modes, where the evaporator and condenser section are orientated parallel to its length. Based on this heating mode, the CLFP-OHP has been shown to efficiently manage the heat loads, and operate with the lower heat load. In the heat transferring mode, the CLFP-OHP is now tasked with transferring heat both axially and across its thickness, through its channels. There have been limited published investigations of the CLFP-OHP application operating in the heat transferring mode. The CLFP-OHP has the potential to be widely used for the cooling of electronic components. As per results obtained in previous researches, the CLFP-OHP is a very favorable technology for achieving effective heat removal rates and uniform temperature on systems. Thus, the current research investigates the applicability of a CLFP-OHP for use as a heat transferring device in electronic applications. This investigation will help in further characterizing CLFP-OHP as the MC-HS for its future use in thermal management.

2 Implementation Methodologies of Minichannel Heat Sink (MC-HS)

The MC-HS comprises a base, a CLFP-OHP developed on the base, and a thin sheet. The MC-HS can be better understood by Fig. 2. The device further comprises a plurality of cooling fins extending outwardly in both directions transverse to the plane of the cooling device. The heat produced by an electronic components such as IGBT, Mosfet, and Diode is dissipated into the atmosphere through the cooling fins. The MC-HS comprises minichannels that carry working fluid. The CLFP-OHP is further divided into an evaporation section, an adiabatic section, and a condenser section in such a manner that the substrates of one or more electronic components are attached to the device at the evaporation section, and the cooling fins are attached to the condensation section. The heat produced by electronic components evaporates working fluid in the evaporation section. The increased temperature and pressure at the evaporation section transfer the working fluid toward the condensation section via the adiabatic section in the form of liquid slugs and vapor plugs. In the condenser section, the temperature and pressure decrease, and liquid slugs and vapor plugs move back toward the evaporation section to continue the evaporation–condensation cycle, whereas the heat is dissipated to the atmosphere via cooling fins.

This oscillatory movement of working fluid and provision of cooling fins optimizes heat dissipation with lower heat transfer resistance. The MC-HS carries working fluid through the minichannels machined at the top of the base. The minichannels of the MC-HS are sealed by a thin sheet. The thin sheet and base are made up of highly conductive material such as aluminum. The thin sheet is brazed to the top of the base to form MC-HS. Here, it is to be noted that the mini channels of the MC-HS are machined on the top of the base by using a vertical milling machine.

2.1 Hydraulic Radius of Minichannel Heat Sink (MC-HS)

The hydraulic radius of minichannels is kept to be small enough so that the liquid slugs and vapor plugs can be developed in the minichannels of the MC-HS. The maximum radius of the channel in MC-HS is given by the Bond number (Bo) (Mehta et al. 2020c, 2019; Khandekar et al. 2002; Kim and Kim 2020a; Srikrishna et al. 2019) as follows:

$$\mathrm{Bo} = \frac{\mathrm{g}(\rho\mathrm{l} - \rho\mathrm{v})\mathrm{r_{h,max}}^2}{\sigma} \tag{1}$$

The bond number is defined as the ratio of gravitational and surface tension forces. Rearranging Eq. (1), the maximum hydraulic radius of the channel for MC-HS can be found as follows:

$$r_{h,max} \leq \sqrt{\frac{\sigma \mathrm{Bo}}{\mathrm{g}(\rho\mathrm{l} - \rho\mathrm{v})}} \tag{2}$$

It is widely reported that if $\mathrm{Bo} \leq 2$, the effect of the surface tension force of working fluid dominates over that of gravitational force (Mehta et al. 2020a, b). In the present investigation, acetone is used as a working fluid.

Table 1 Summary of CLFP-OHP experimental researches

Type of research	Researchers	Driving fluid	Evaporator area (mm^2)	Condenser area (mm^2)	Number of channel	Ares of channel (mm^2)	Heat load (watt)	Filling ratio (%)
Experimental	Khandekar et al. (2002)	Water	30 × 22	30 × 13	12	2.2 × 2	25–70	25
/Visualization		Ethanol						30
								70
Experimental	Yang et al. (2004)	Ethanol	100 × 30	100 × 60	40	2 × 2	10–200	90
Experimental	Qu and Yang (2009)	Acetone	20 × 60	100 × 60	22	1.5 × 1.5	10–100	50
								20.90
Experimental	Chang et al. (2010)	Acetone	25.4 × 25.4	25.4 × 90	16	0.762 × 0.762	10–140	70
		Water			10	1 × 1		
		Nano fluids			8	1.7 × 1.175		
						1.75 × 1.17		
Experimental	Thompson and Ma (2010)	Acetone	63.5 × 31.75	76.2 × 76.2	15	0.762 × 0.762	10–180	7
Experimental/ Visualization	Chien et al. (2011)	Distilled water	15 × 40	40 × 40	8	2 × 2	140	40
								50
								60
								70
Experimental	Lefevre et al. (2012)	Methanol	190 × 90	30 × 90	8	4 × 4	80	70
		FC-72						
Type of research	**Investigators**	**Working fluid**	**Evaporator size (mm^2)**	**Condenser size (mm^2)**	**Number of channel**	**Size of channel (mm^2)**	**Heat load (watt)**	**Charge ratio (%)**
Experimental	Failed (2014)	Water	83 × 32	82.5 × 31.75	10	2 × 2	10–100	75
Experimental	Laun et al. (2015)	Acetone	80 × 30	15 × 30	20	1.3 × 1.3	50–500 W	80
Experimental	Hao et al. (2014)	DI Water	57 × 28	57 × 36	6	2 × 2	50–80	55
Experimental	Thompson et al. (2014)	Acetone	30 × 30	30 × 30	15	1.02 × 1.02	50–250 W	80
Experimental	Manno et al. (2015)	Ethanol	105 × 45	125 × 67	10	2 × 2	10–100	50
/Visualization								
Experimental	Ayel et al. (2015)	FC-72	10 × 120	200 × 120	12	1.6 × 1.7	30 -180	50
Experimental	Zhang et al. (2016)	HPLC water	25 × 40	30 × 40	10	1 × 1.5	75–225	65
Experimental	Lee and Kim (2017)	FC-72	10 × 16	15 × 16	5	2 × 2	50	50
/Visualization								
Experimental	Jang et al. (2017)	FC-72	25 × 54	25 × 54	5	2 × 2	5–28	70
/Visualization								
Experimental	Kim and Kim (2020a)	R-134a	24 × 53.5	24 × 53.5	20	0.6 × 2	4–48	50
/Visualization		Ethanol						

Table 1 (continued)

Type of research	Investigators	Working fluid	Evaporator size (mm^2)	Condenser size (mm^2)	Number of channel	Size of channel (mm^2)	Heat load (watt)	Charge ratio (%)
Experimental	Kim and Kim (2020b)	Ethanol	20×35	20×35	10	0.5×1	9–31	50
		FC-72						
		HFE-7000						
		R-134a						
Experimental	Yoon and Kim (2017)	Ethanol	10×18	18×18	5	1×0.5	5–20	55
/Visualization								
Experimental	Kim and Kim (2018)	Ethanol	10×18.5	15×18.5	10	10×18	2–16	50%
/Visualization								
Experimental	Alijani et al. (2018)	Isopropyl alcohol	14×28	20×20	50	0.2×0.2	2.1–5.3	30
					26	0.4×0.4		
					13	0.8×0.8		
					7	1.6×1.6		
Experimental	Wits et al. (2018)	Water	50×50	50×50	12	2.2×2	20–100	40
		Methanol						
		Ammonia						
Experimental	Stevens et al. (2019)	Butane	12×12	24×64	34	1×1	10–40	46
Experimental	Cecere et al. (2018)	R134a	120×10	100×140	11	3×3	0–200	50
/Visualization		WaterSelf-rewetting mixture						
Experimental	Liang et al. (2018)	Ionic liquids	57×28	57×36	8	2×2	50–250	67
/Visualization		Water						
Experimental	Yoon and Kim (2019)	Ethanol	10×18.5	15×18.5	10	1×0.5	2–26	55
/Visualization								
Experimental	Jo et al. (2019)	Ethanol	10×28	10×28	10	1.6×1.6	2–16	50
/Visualization								
Experimental	Takawale et al. (2018)	Ethanol	32×101.4	65×101.4	34	1.2×1.2	20–180	40
/Visualization								60
								80
Experimental	Jang et al. (2018)	FC-72	25×54	25×54	28	0.82×0.3	1.5–5	50
					20	1.55×0.3		
					12	3.25×0.3		
					16	0.82×0.3		
					16	1.55×0.3		
Experimental	Ayel et al. (2018)	FC-72	10×120	160×120	22	2.5×2.5	20–150	50
/Visualization								
Experimental	Jun and Kim May (2019)	Ethanol	10×33.5	15×33.5	20	1×0.5	16–24	47
/Visualization								

Table 1 (continued)

Type of research	Investigators	Working fluid	Evaporator size (mm^2)	Condenser size (mm^2)	Number of channel	Size of channel (mm^2)	Heat load (watt)	Charge ratio (%)
Experimental	Al-Zaidi et al. (2018)	HFE-7100	20×25	20×25	15	1×0.4	10–50	48
/Visualization								
Experimental	Lim and Kim (2019)	HFE-7100	15×15	15×33.5	20	0.5×0.5	5–12	50
Experimental	Qu et al. (2019)	Ethanol	30×15	65×15	18	1.5×1.8	0–200	50
/Visualization								
Experimental	Kearney et al. (2016)	Novec 649	50×10	50×10	44	1.5×1.9	0–50	30
		Novec 774						40
								50
								70

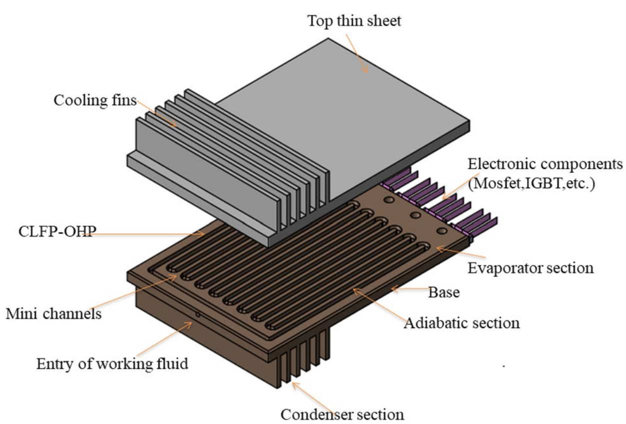

Fig. 2 MC-HS

Table 2 Properties of acetone at 20 °C and 1 atm (Mehta et al. 2020a)

Property	Acetone
Boiling point (°C)	56
Surface tension (N/m)×10^{-3}	23.7
Liquid density (Kg/m^3)	790
Vapor density	0.64
Liquid specific heat (KJ/Kg°C)	2.16
Dynamic viscosity (Pa-sec)×10^{-3}	0.32

The thermophysical properties of acetone are presented in Table 2. This investigation used a Bo of 2, as reported in the previous study (Wits et al. 2018; Shafii et al. 2001).

As per Eq. (2), the $r_{h,max}$ is 2.47 mm for acetone as a working fluid. To achieve high thermal performance with the working fluid, the maximum hydraulic radius of the channel of water and acetone is compared. According to Eq. (2), the $r_{h,max}$ of MC-HS was plotted in Fig. 3 in the temperature range from 20 to 140 °C. Both for acetone and water, the r_h, max decreases with the temperature increase but the acetone have a smaller one. At 140 °C, their $r_{h,max}$ values are 1.64 and 3.34 mm, respectively. To investigate the thermal performance of the MC-HS, a square 2×2 mm^2 channel was used in the investigation to make sure liquid slugs and vapor plugs could be formed inside the minichannel. The hydraulic radius of the 2×2 mm^2 square channel is within the range of calculated r_h, max. The evaporator section, condenser section, and adiabatic section were 30×70 mm^{2,} respectively. The charge tube was used to charge the working fluid in the MC-HS. The MC-HS was arranged in a sandwiched manner between the base and the thin sheet. As shown in Fig. 4, the condenser section includes cooling fins transversely extended from both the base and thin sheet

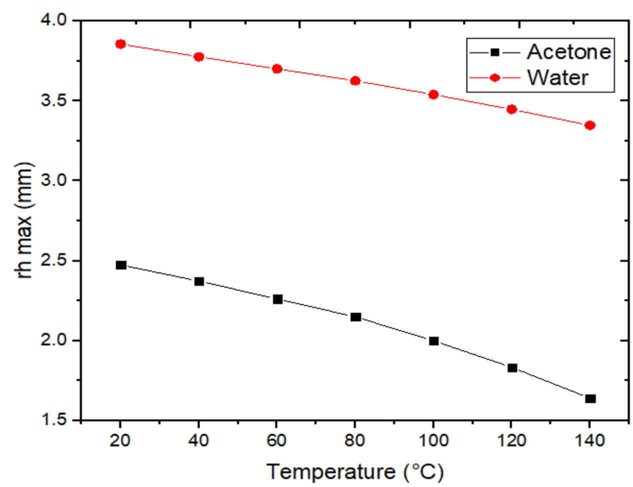

Fig. 3 r_h, max versus temperature for water and acetone

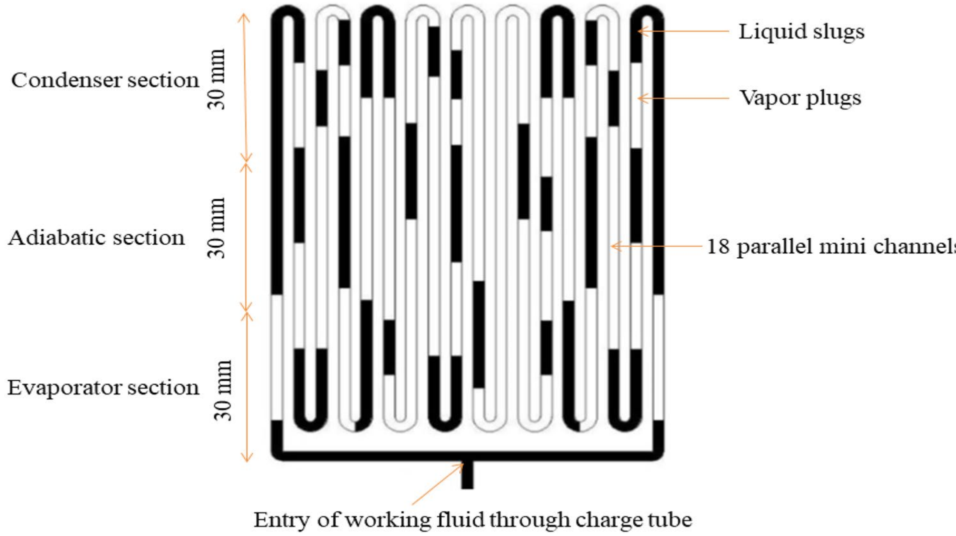

Fig. 4 Oscillatory motion in MC-HS

outwardly for dissipating heat produced by the electronic components in the atmosphere.

2.2 Fabrication of Minichannel Heat Sink (MC-HS)

Figure 4 shows the two-phase flow in the form of liquid slugs and vapor plugs in the MC-HS. As shown in Fig. 4, the MC-HS is configured to carry the working fluid in the form of liquid slugs and vapor plugs in a closed-loop configuration. The MC-HS is provided with a charge tube at the condenser section to charge the MC-HS with working fluid. The hole is drilled to the base to braze the charge tube to the minichannels. To realize this, MC-HS is first evacuated with the help of a mechanical vacuum pump and then is charged with the working fluid via a charge tube.

The minichannel structure was machined onto the base of the device as shown in Fig. 5a and b shows the assembly of a MC-HS. During operation, the heat from electronic components is received by the evaporator section of the MC-HS. This evaporates the working fluid and converts it into the liquid slugs and the vapor plugs that flow in minichannels. The evaporation phenomena that occurred in the evaporation section raised the temperature and vapor pressure in this section. This causes the liquid slugs and the vapor plugs to flow toward the condenser section through the adiabatic section of the MC-HS. At the condenser section, the temperature and pressure of the vapor plugs drop and the vapor plugs start condensing. The heat carried by the liquid slugs and the vapor plugs is dissipated in the condenser section using cooling fins. The condensation further drops the vapor pressure of the working fluid and hence the fluid flows back toward the evaporator section. The cycle of evaporation and condensation continues and the oscillating flow is developed in the MC-HS. As a result of the oscillation of the liquid slugs and vapor plugs, the heat of electronic components

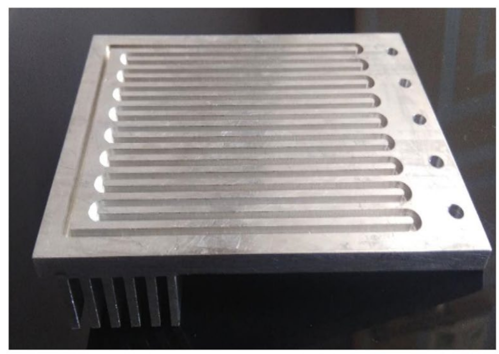

(a) Base with CLFP-OHP structure

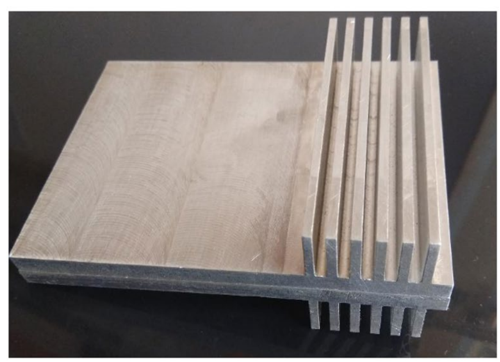

(b) Assembly of MC-HS

Fig. 5 CLFP-OHP embedded in the MC-HS

is continuously transferred from the evaporator section to the condenser section. In the MC-HS, due to the oscillatory flow of the liquid slugs and vapor plugs inside the MC-HS, reduces the thermal resistance experienced in the heat transfer. In this way, a higher thermal resistance problem of conventional heat sink cooling methods is overcome which makes the MC-HS to be more suitable for the dissipation of the heat produced by electronic components. The MC-HS is placed vertically, i.e., perpendicular to the printer circuit board on which the electronic component is mounted, to optimize the oscillatory motion of working fluid so that the liquid slugs and vapor plugs circulate more smoothly in the minichannels and enhance the operating range of the MC-HS.

3 Experimental Apparatus of MC-HS

The experimental setup of the MC-HS is depicted in Fig. 6. The experimental setup is comprised of the MC-HS, a power supply system, an air supply system, the temperature scanner, the RS485 USB converter, and the personal computer. The objective of the experimental setup is to characterize the thermal performance of the MC-HS for variation in applied heat load at the evaporator section. The MC-HS was fabricated with a CLFP-OHP structure. The MC-HS has 18 parallel channels with a length of 90 mm and 9 turns with a hydraulic radius of the channel of 2.44 mm, which created a closed-loop FP-OHP. The MC-HS is made of aluminum. The area of the MC-HS is $90 \times 70 \times 5$ mm^3.

The area of the evaporator section, adiabatic section, and condenser section was 30×70 mm^{2,} respectively. In addition, to minimize the thermal contact resistance between the heaters and the evaporator section, thermally conductive paste was put between the heater and the surface. Based on the experimental observation in the previous research, various parameters of the MC-HS were selected and listed in Table 3.

The experimental apparatus of the MC-HS is depicted in Fig. 7. The setup also allows the acquisition of temperature measurements during operation. The temperatures were measured by K-type thermocouples and collected by the temperature scanner then the data interfaced with

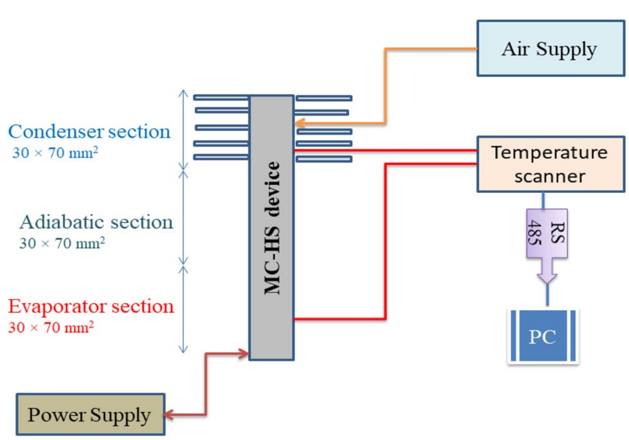

Fig. 6 MC-HS experimental setup

Table 3 MC-HS parameters

Charge Ratio	Orientation	Channel size	Channel shape	Working fluid
60%	Vertical	2×2 mm^2	Square	Acetone

the personal computer via RS 485 USB converter. In order to obtain temperatures of acetone inside the MC-HS test section simultaneously, six K type thermocouples with an accuracy of 0.1 °C were inserted into small holes drilled by the machining method at different locations along the edge channel of the evaporator section and condenser section of the device. The assembly was wrapped in insulation to reduce heat losses to the ambient. During testing, the electrical power (10–40 W) to the evaporator section was regulated by a variable transformer monitored by ammeter and voltmeter. The condenser section of was cooled by air at an ambient temperature of 1 ± 30 °C. Prior to operation, the MC-HS is evacuated and then partially charged with the de-gassed working fluid. Precise charging of the device is achieved using a syringe. When the acetone enters the device, it orientates itself naturally into a series of liquid slugs and vapor plugs inside the minichannels due to the dominance of surface tension forces.

4 Uncertainty Analysis

The uncertainties analysis of the MC-HS has been calculated by Moffat (Moffat 1985) and Kline and McClintock method (Kline 1953). The thermal performance, an important parameter of the MC-HS is calculated from Eq. (3).

$$R_{\mathrm{th}} = \frac{T_{\mathrm{e}} - T_{\mathrm{c}}}{Q} \quad (3)$$

where T_e, $T_{c,}$ and Q are the average temperatures of the evaporator, condenser, and heat load, respectively.

$$T_e = \frac{1}{4}\sum_{i=1}^{4} T_i$$

$$T_c = \frac{1}{4}\sum_{i=1}^{4} T_i$$

The parameters that contributed significantly to the uncertainty of thermal resistance are listed in Table 4. The uncertainty analysis of MC-HS is as follows.

According to the uncertainty analysis method, the input power for the MC-HS can be calculated by multiplying U and I expressed as follows:

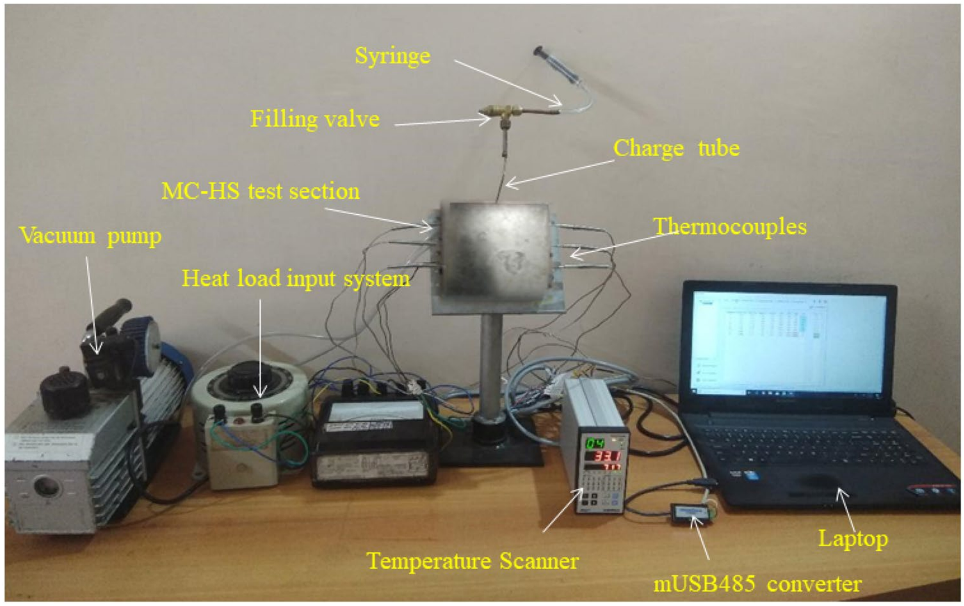

Fig. 7 MC-HS experimental apparatus

Table 4 Uncertainty of the main parameters

Parameters	Accuracy
Evaporator temperature	±0.5 °C
Condenser temperature	±0.5 °C
Voltage	0.1%
Current	0.1%
Thermal resistance	4.26%

$$Q = U \times I \tag{4}$$

The uncertainties can be expressed:

$$\frac{\partial Q}{Q} = \sqrt{\left(\frac{dU}{U}\right)^2 + \left(\frac{dI}{I}\right)^2} \tag{5}$$

$$\frac{\partial R}{R} = \sqrt{\left(\frac{\delta T_e}{T_e - T_c}\right)^2 + \left(\frac{\delta T_c}{T_e - T_c}\right)^2 + \left(\frac{\delta Q}{Q}\right)^2} \tag{6}$$

The voltage and current of heat load input system have accuracies both of 0.5. For 10 W, the detailed measured data are: U = 30 V, I = 0.33 A, T_e-T_c = 30 °C (Acetone, charge ratio = 60%); then.

$$\frac{\partial Q}{Q} = \sqrt{\left(\frac{0.5\% \times 80}{30}\right)^2 + \left(\frac{0.5\% \times 1}{0.3}\right)^2} = 2.31\% \tag{7}$$

$$\frac{\partial R}{R} = \sqrt{\left(\frac{0.5}{30}\right)^2 + \left(\frac{0.5}{30}\right)^2 + (2.13)^2} \tag{8}$$

Selected coverage factor (K) as 2, then maximum uncertainty ($\varnothing_{max}$) is:

$$\varnothing\text{max} = K \times \frac{\partial R}{R} = 2.12\% \times 2 = 4.25\% \tag{9}$$

This is the maximum one for its small heat load and small temperature difference.

5 Results and Discussion

The objective of this research was to investigate the thermal performance of the MC-HS for use in electronic cooling. The performance enhancement due to MC-HS was determined by subtracting the heat loss to the environment and heat transfer through the MC-HS from the heat load input.

5.1 Temperature Responses of Evaporator and Condenser Section

The geometry of MC-HS plays a significant role in thermal performance which greatly affects the distribution of working fluid and the transition of flow patterns, especially when the cross-sectional shape is not circular, such as rectangular, the effect of the angled corners on the flow patterns is more obvious (Zhang et al. 2021). The start-up process of MC-HS involves the onset of two phase flow oscillations for the estimation of the thermal performance of MC-HS at low heating load. The startup characteristic of the MC-HS is indicated by the variation of the temperature at the evaporator section.

The measured evaporator temperature data for the MC-HS at 10 W are displayed in Fig. 8. At 10 W, the evaporation process was relatively weak in the evaporator section,

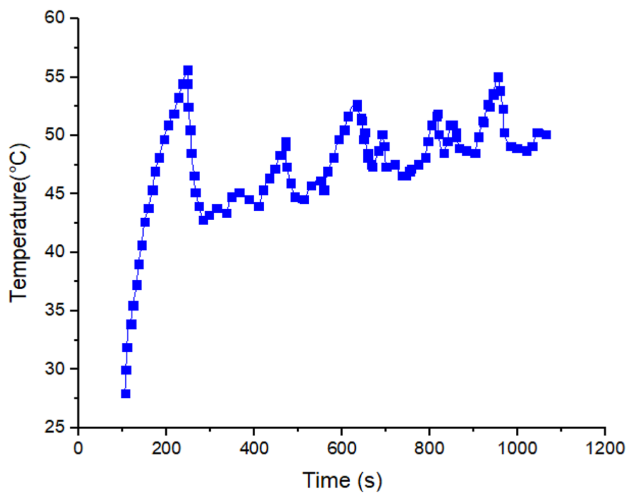

Fig. 8 The startup characteristics of MC-HS at 10 W

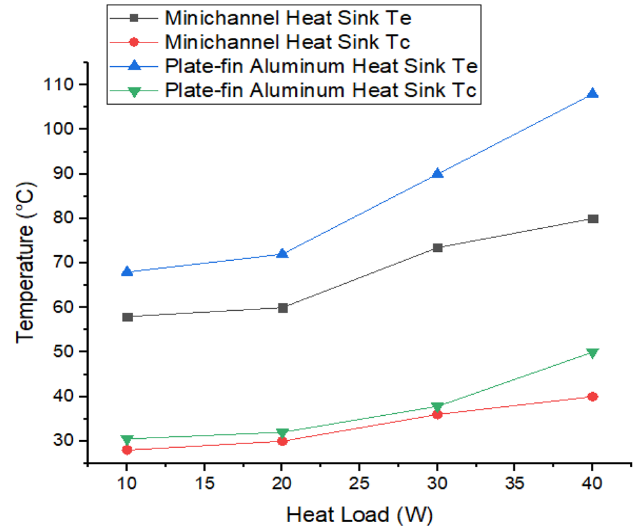

Fig.9 Temperature responses of evaporator and condenser section

and thus the generated vapor plugs were insufficient and the liquids slugs moved slowly, resulting in the low-frequency and large-amplitude characteristics. With the assistance of the gravity force, the MC-HS started up easily for vertical (90°) orientation. And the startup time and temperature were 57 °C and 225 s, respectively. At an increased heat load, the working fluid in the MC-HS is involved in the minichannel, and the faster fluid flow in the device results in a shorter startup time. Low heat load and short start-up time indicate rapid and sensitive thermal responses, which are required for electronic cooling applications (Xu et al. 2019; Sagar et al. 2022).

After heating for a certain period, the temperature difference between the evaporator section and condenser section provides a sufficient driving force for the oscillation motion of the working fluid. The operation characteristic of the MC-HS is indicated by the variation of the temperatures at the evaporator section and condenser section. The temperature responses of the evaporator and condenser sections are presented in Fig. 9 with the corresponding performance of the plate-fin aluminum heat sink when the heat load was increased from 10 to 40 W. In all tests, the maximum heat load given by the heat load input system was 40 W, and the heat dissipated through the cooling fins which were cooled by incoming air. The heat sink was tested repeatedly to set a baseline for the MC-HS performance. Both the plate-fin aluminum heat sink and MC-HS s had similar boundary conditions. For all heat loads investigated, the MC-HS provides a lower evaporative temperature relative to the solid heat sink. The percentage reduction in evaporator temperature, when using the cooling device is varied between 14 and 25%, depending on the heat load. On the other hand, the MC-HS device had minimal temperature improvement across its surfaces compared to the solid heat sink.

5.2 Comparison of Temperature Difference of MC-HS and Heat Sink

As indicated in Fig. 10, with the increasing heat load, the temperature difference between the evaporator section and the condenser section becomes larger. This is an expected result as the heat transfer amount is increased if the heat load is larger. From Fig. 10, the MC-HS had 18 °C lower temperature difference than the heat sink at 40 W. It is observed that the temperature difference between the evaporator and condenser section for the MC-HS is smaller than that for a plate-fin aluminum heat sink at the same heat load. For example, when the heat load is 40 W, the temperature difference for the heat sink is about 58 °C while for the MC-HS it

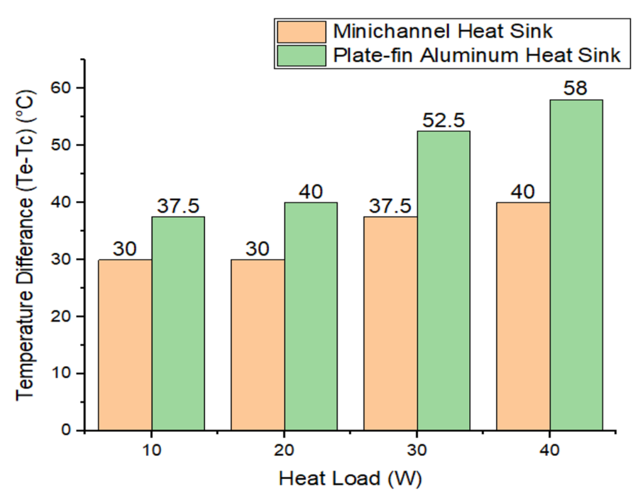

Fig. 10 Comparison of temperature difference of MC-HS and Heat Sink

is 40 °C. This observation indicates that the MC-HS is better than a plate-fin aluminum heat sink in terms of heat transfer capability. The oscillatory motions of liquid slugs and vapor plugs are evident in the temperature profiles of the MC-HS. The heat sink embedded with minichannels essentially utilizes the changes in the temperature and pressure during the expansion and contraction of volume in the process of phase changes to stimulate the oscillation motion of liquid slugs and vapor plugs in the minichannels.

The MC-HS was able to maintain an operational temperature for the electronic component even with 40 W heat loads. At an increased heat load, more fluid in the CLFP-OHP is involved in the MC-HS working cycle, and the faster oscillatory flow in the device results in a reduction in temperature difference and hence improvement in thermal performance.

The temperature difference between the evaporator and condenser sections indicates the oscillatory motion of working fluid in the device. The experimental results indicated that the MC-HS achieved a steady state condition through natural convection cooling. The heat load accumulation made the saturation pressure high enough to drive the oscillatory motion of liquid slugs and vapor plugs, and the working fluid from the bottom was pushed to the condenser section.

5.3 Thermal Performance of MC-HS

The thermal performance of the MC-HS is evaluated by the thermal resistance. The temperature difference between the evaporator and condenser section is very important for justifying the thermal performance of the MC-HS. If Rth is calculated to be a smaller value, the heat transfer capability of the MC-HS is better. The obtained thermal resistance values of both heat sink and MC-HS s are plotted in Fig. 11.

It indicates that the thermal resistance decreases with an increase in the heat load. The results indicate that the thermal resistance of the MC-HS varies from 3 °C/W to 1 °C/W when the heat load changes from 10 to 40 W. The thermal resistance for a MC-HS is generally 20–31% smaller than that of the plate-fin aluminum heat sink at the same heat load. For the 10 W heat load, the plate-fin aluminum heat sink has a thermal resistance of 3.75 °C/W, while the thermal resistance of the MC-HS is 3 °C/W, reduced by 20%. For the other heat loads, 30–40 W, the thermal resistance of the MC-HS is reduced by 28.16–31.03%, respectively, if the plate-fin aluminum heat sink is replaced by the MC-HS.

Compared with a plate-fin aluminum heat sink, the fluid of the MC-HS is divided into many relatively minichannels by the closed-loop structure; the oscillatory motion of liquid slugs and vapor plugs in minichannel reduces thermal resistance. It is found that the minichannels have proper flow circulation and are easier to form a circulating flow of working fluid. Particularly, the square channels can generate more

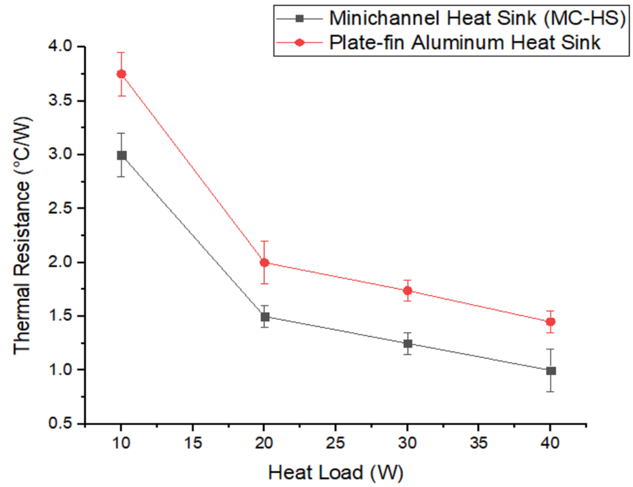

Fig. 11 Thermal performance comparison of MC-HS and plate-fin aluminum heat sink

driving force, which consequently increases the flow velocity of the working fluid and improve the thermal performance of the MC-HS. For the MC-HS, the nonuniform distribution of liquid slugs and vapor plugs makes the pressure distribution inside the minichannels uneven, which is easier to form two phase heat transfer. By comparing the MC-HS with the conventional heat sink, experimental results show that the MC-HS has a more intense self-excited oscillation motion of working fluid. Therefore, it can increase the flow velocity of the working fluid and increase the thermal performance of the MC-HS. Working fluid acts an essential role in the thermal performance of MC-HS, which directly determines the operating range of the device. The latent heat and boiling point of acetone are lower, which are beneficial to the evaporation of the evaporator section and the condensing of the condenser section (Kim and Kim 2020b). Therefore, it would increase the pressure difference between the evaporator section and the condenser section. Consequently, the low dynamic viscosity of acetone is beneficial to the oscillatory flow of the working fluid (Kim and Kim 2020a). In addition, the cooling fins enlarged the condenser surface area and increased the thermal performance of the MC-HS. Hence the thermal resistance of a MC-HS should easily surpass a plate-fin aluminum heat sink device. The MC-HS technology is maturing as a real world thermal management solution for electronics systems. Recent advancements in manufacturing have enabled MC-HS to be embedded inside a wide range of conventional cooling techniques.

5.4 Model Validation

To check the validity of the minichannel heat sink, verification was made by comparing the results with the experimental data of Mehta et al. (Mehta et al. 2020a). The geometric

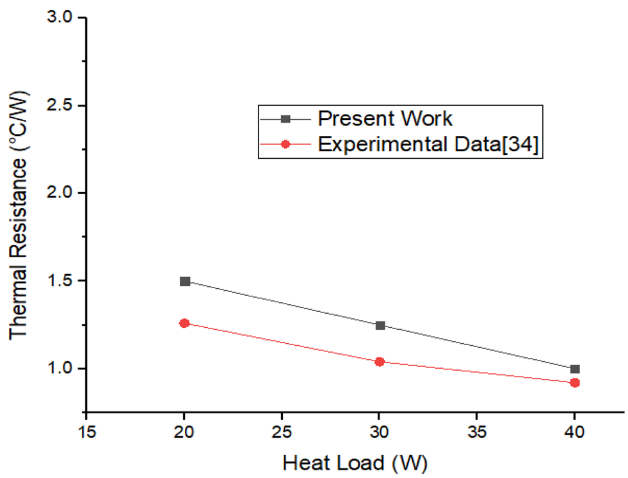

Fig. 12 Comparison with experimental results

parameters of the MC-HS are substantially the same as that of the literature, and the charge ratio is set as 60%. Figure 12 compares the present results with the experimental data for acetone. In Fig. 12, the maximum deviation of thermal resistance from the experimental data is 4.2%. Therefore, it can be seen that the present results are in a good agreement with the experimental data.

6 Conclusions

A new enhanced model is investigated to improve the thermal performance of conventional plate-fin aluminum heat sinks. Compared with the conventional plate-fin aluminum heat sink, the new MC-HS has 18 parallel minichannels machined on the aluminum base plate, which forms more pathways for working fluid to oscillate between the evaporator section and the condenser section. The MC-HS was oriented vertically and the evaporator section was used to give heat load up to 40 W. According to the results, it is concluded that the MC-HS is an effective method in the thermal management of electronic devices, which has the following advantages.

- The MC-HS with 2×2 mm^2 square channels and charged with acetone achieved thermal resistance of 1 °C/W.
- Compared to the plate-fin heat sink, the enhanced model was better due to two phase heat transfer occurred in minichannels. The MC-HS can operate in the heat spreading configuration, as evidenced by temperature responses of the evaporator and condenser sections changes with the heat load.
- Experimental results show that the thermal resistance of the MC-HS is reduced by 20–31%. The MC-HS can reduce the temperature difference between 14 and 25%.
- The proposed methods in this study guarantee the lower thermal resistance required in the electronic devices.

The thermal resistance is decreased with an increase in the heat load. The experimental results indicate the new MC-HS is more superior for the high dissipation of the electronic components.

7 Future Work

In future work, the dispersion of nano-sized particles in the working fluid could be the better choice for enhancing the heat transfer capability of MC-HS. The correlation of different performance parameters can be established in future research work so that more insight into the operating characteristics of MC-HS is understood.

Funding All authors certify that they have no affiliations with or involvement in any organization or entity with any financial interest or non-financial interest in the subject matter or materials discussed in this manuscript. This article was funded by Student Start-up and Innovation Policy (SSIP), 201921003211, Kamlesh Mehta

Declarations

Conflict of interest The authors have no competing interests to declare that are relevant to the content of this article.

References

Al-Zaidi AH, Mahmoud MM, Karayiannis TG (2018) Condensation flow patterns and heat transfer in horizontal microchannels. Exp Thermal Fluid Sci 90:153–173

Alijani H, Çetin B, Akkuş Y, Dursunkaya Z (2018) Effect of design and operating parameters on the thermal performance of aluminum flat grooved heat pipes. Appl Therm Eng 132:174–187

Arshad W, Ali HM (2017) Graphene nanoplatelets nanofluids thermal and hydrodynamic performance on integral fin heat sink. Int J Heat Mass Transf 107:995–1001

Ayel V et al (2015) Experimental study of a closed loop flat plate pulsating heat pipe under a varying gravity force. Int J Therm Sci 96:23–34

Ayel V, Araneo L, Marzorati P, Romestant C, Bertin Y, Marengo M (2019) Visualization of flow patterns in closed loop flat plate pulsating heat pipe acting as hybrid thermosyphons under various gravity levels. Heat Transf Eng 40(3–4):227–237

Bao-Min L (2004) Multi-physics simulation of a microprocessor package under water cooling. J Electron Packag 126(3):384–389

Bedi N, Subbarao PMV (2021) Experimental study of backward conduction in multi-microchannel heat sink. Iran J Sci Technol Trans Mech Eng 45(4):1021–1031

Cecere A et al (2018) Experimental analysis of a flat plate pulsating heat pipe with self-rewetting fluids during a parabolic flight campaign. Acta Astronaut 147:454–461

Chamanroy Z, Khoshvaght-Aliabadi M (2019) Analysis of straight and wavy miniature heat sinks equipped with straight and wavy pin-fins. Int J Therm Sci 146:106071

Cheng P, Thompson S, Boswell J, Ma H (2010) An investigation of flat-plate oscillating heat pipes. J Electron Packag 132(4):041009–041016

Chien K, Chen Y, Lin Y, Wang C and Yang K (2011) The experimental studies of flat-plate closed-loop pulsating heat pipes. In: The tenth international heat pipe symposium, Taipei, Taiwan, pp 212–216

Fairley JD, Thompson SM, Anderson D (2015) Time–frequency analysis of flat-plate oscillating heat pipes. Int J Therm Sci 91:113–124

Ghasemi SE, Ranjbar AA, Hoseini SMJ (2018) Cooling performance analysis of water-cooled heat sinks with circular and rectangular minichannels using finite volume method. Iran J Chem Chem Eng (IJCCE) 37(2):231–239

Ghasemi S, Ranjbar A, Hoseini M, Mohsenian S (2021) Design optimization and experimental investigation of CPU heat sink cooled by alumina-water nanofluid. J Market Res 15:2276–2286

Ghasemi SE, Ranjbar A, Hosseini M (2017a) Forced convective heat transfer of nanofluid as a coolant flowing through a heat sink: experimental and numerical study. J Mol Liq 248:264–270

Ghasemi SE, Ranjbar A, Hosseini M (2017b) Numerical study on the convective heat transfer of nanofluid in a triangular minichannel heat sink using the Eulerian-Eulerian two-phase model. Numer Heat Transf Part a: Appl 72(2):185–196

Ghasemi SE, Ranjbar A, Hosseini M (2017c) Thermal and hydrodynamic characteristics of water-based suspensions of Al2O3 nanoparticles in a novel minichannel heat sink. J Mol Liq 230:550–556

Ghasemi SE, Ranjbar A, Hosseini M (2017d) Experimental and numerical investigation of circular minichannel heat sinks with various hydraulic diameter for electronic cooling application. Microelectron Reliab 73:97–105

Ghasemi SE, Ranjbar A, Hosseini M (2017e) Numerical study on effect of CuO-water nanofluid on cooling performance of two different cross-sectional heat sinks. Adv Powder Technol 28(6):1495–1504

Ghasemi SE, Ranjbar A, Hosseini M (2017f) Experimental evaluation of cooling performance of circular heat sinks for heat dissipation from electronic chips using nanofluid. Mech Res Commun 84:85–89

Gholinia M, Ranjbar A, Hosseinpour A (2022) CFD analysis of (TiO2)–H2O Nanofluids on Si-IGBT power electronic module with a new micro-nozzle model. J Therm Anal Calorim 147:1–13

Gholinia M, Ranjbar A, Javidan M, Hosseinpour A (2021) Employing a new micro-spray model and (MWCNTs-SWCNTs)-H2O nanofluid on Si-IGBT power module for energy storage: a numerical simulation. Energy Rep 7:6844–6853

Gholinia M, Ranjbar A, Javidan M, Hosseinpour A (2022b) Effect of two different nano-particles (GO-MoS2) and a new micro-sprayer model on power electronic module for thermal management. Adv Mech Eng 14(5):16878132221087512

Gnanadurai RR, Varadarajan A (2016) Investigation on the effect of cooling of the tool using heat pipe during hard turning with minimal fluid application. Eng Sci Technol Int J 19(3):1190–1198

Hao T, Ma X, Lan Z, Li N, Zhao Y (2014) Effects of superhydrophobic and superhydrophilic surfaces on heat transfer and oscillating motion of an oscillating heat pipe. J Heat Transfer 136(8):082001–082013

Hashemi SMH, Fazeli SA, Zirakzadeh H, Ashjaee M (2012) Study of heat transfer enhancement in a nanofluid-cooled miniature heat sink. Int Commun Heat Mass Transfer 39(6):877–884

He Y, Jiao D, Pei G, Hu X, He L (2020) Experimental study on a three-dimensional pulsating heat pipe with tandem tapered nozzles. Exp Therm Fluid Sci 119:110201

Hoesing MP and Michna GJ (2014) Integration of a Pulsating Heat Pipe in a Flat Plate Heat Sink," In: ASME 2014 12th International conference on nanochannels, microchannels, and minichannels, Am Soc Mech Eng

Hosseinirad E, Khoshvaght-Aliabadi M, Hormozi F (2019) Effects of splitter shape on thermal-hydraulic characteristics of plate-pin-fin heat sink (PPFHS). Int J Heat Mass Transf 143:118586

Jang DS, Lee JS, Ahn JH, Kim D, Kim Y (2017) Flow patterns and heat transfer characteristics of flat plate pulsating heat pipes with various asymmetric and aspect ratios of the channels. Appl Therm Eng 114:211–220

Jang DS, Kim D, Hong SH, Kim Y (2019) Comparative thermal performance evaluation between ultrathin flat plate pulsating heat pipe and graphite sheet for mobile electronic devices at various operating conditions. Appl Therm Eng 149:1427–1434

Jo J, Kim J, Kim SJ (2019) Experimental investigations of heat transfer mechanisms of a pulsating heat pipe. Energy Convers Manage 181:331–341

Jun S, Kim SJ (2019) Experimental investigation on the thermodynamic state of vapor plugs in pulsating heat pipes. Int J Heat Mass Transf 134:321–328

KavoosiBalotaki H, Saidi MH (2019) Design and performance of a novel hybrid photovoltaic-thermal collector with pulsating heat pipe (PVTPHP). Iran J Sci Technol Trans Mech Eng 43(1):371–381

Kearney DJ, Suleman O, Griffin J, Mavrakis G (2016) Thermal performance of a PCB embedded pulsating heat pipe for power electronics applications. Appl Therm Eng 98:798–809

Khandekar S, Schneider M, Schafer P, Kulenovic R, Groll M (2002) Thermofluid dynamic study of flat-plate closed-loop pulsating heat pipes. Microscale Thermophys Eng 6(4):303–317

Kim W, Kim SJ (2018) Effect of reentrant cavities on the thermal performance of a pulsating heat pipe. Appl Therm Eng 133:61–69

Kim W, Kim SJ (2020a) Effect of a flow behavior on the thermal performance of closed-loop and closed-end pulsating heat pipes. Int J Heat Mass Transf 149:119251

Kim J, Kim SJ (2020b) Experimental investigation on working fluid selection in a micro pulsating heat pipe. Energy Convers Manage 205:112462

Kline SJ (1953) Describing uncertainty in single sample experiments. Mech Eng 75:3–8

Laun F, Lu H, Ma H (2015) An experimental investigation of an oscillating heat pipe heat spreader. J Therm Sci Eng Appl 7(2):2100–2105

Lee J, Kim SJ (2017) Effect of channel geometry on the operating limit of micro pulsating heat pipes. Int J Heat Mass Transf 107:204–212

Lefèvre F, Lips S, Rullière R, Conrardy J-B, Raynaud M, Bonjour J (2012) Flat plate heat pipes: from observations to the modeling of the capillary structure. Front Heat Pipes (FHP) 3(1):1–9

Li Y, Gong L, Ding B, Xu M, Joshi Y (2021) Thermal management of power electronics with liquid cooled metal foam heat sink. Int J Therm Sci 163:106796

Liang Q, Hao T, Wang K, Ma X, Lan Z, Wang Y (2018) Startup and transport characteristics of oscillating heat pipe using ionic liquids. Int Commun Heat Mass Transf 94:1–13

Liang K, Li Z, Chen M, Jiang H (2019) Comparisons between heat pipe, thermoelectric system, and vapour compression refrigeration system for electronics cooling. Appl Therm Eng 146:260–267

Lim J, Kim SJ (2019) Effect of a channel layout on the thermal performance of a flat plate micro pulsating heat pipe under the local heating condition. Int J Heat Mass Transf 137:1232–1240

Liu X, Xu L, Wang C, Han X (2019) Experimental study on thermo-hydrodynamic characteristics in a micro oscillating heat pipe. Exp Thermal Fluid Sci 109:109871

Lu G, Yang J, Zhai X, Wang X (2021) Hotspot thermal management in microchannel heat sinks with vortex generators. Int J Therm Sci 161:106727

Manno V, Filippeschi S, Mameli M, Romestant C, Ayel V, Bertin Y (2015) Thermal-hydraulic characterization of a flat plate pulsating heat pipe for automotive applications. Interfacial Phenom Heat Transf 3(4):413–425

Marcinichen JB, Olivier JA, Lamaison N, Thome JR (2013) Advances in electronics cooling. Heat Transf Eng 34(5–6):434–446

Mehta K, Mehta N (2016) Development of flat plate oscillating heat pipe as a heat transfer device. Front Heat Pipes (FHP) 7(1):1–7

Mehta K, Mehta N, Patel V (2020) Influence of the channel profile on the thermal resistance of closed-loop flat-plate oscillating heat pipe. J Braz Soc Mech Sci Eng 42(3):123

Mehta K, Mehta N, Patel V, Badgujar A, Mehta S, Bora N (2020) Experimental investigation of flat plate cryogenic oscillating heat pipe. J Low Temp Phys 198(1):41–55

Mehta K, Mehta N, Patel V 2019 Effect of Operational parameters on the thermal performance of flat plate oscillating heat pipe. J Heat Transf, 141(12), pp 121802-1-8, 2019

Mehta K, Mehta N, Patel V (2020a) Experimental investigation of the thermal performance of closed loop flat plate oscillating heat pipe. Exp Heat Transf, pp 1–19

Moffat RJ (1985) Using uncertainty analysis in the planning of an experiment. J Fluids Eng 107(2):173–178

Mohsen OA, Muhammed MAR, Hasan BO (2021) Heat transfer enhancement in a double pipe heat exchanger using different fin geometries in turbulent flow. Iran J Sci Technol Trans Mech Eng 45(2):461–471

Mudawar I (2013) Recent advances in high-flux, two-phase thermal management. J Therm Sci Eng Appl 5(2):021012–021015

Qi P, Li X, Qiu F, Qiao S, Tan S, Wang X (2020) Application of particle image velocimetry measurement technique to study pulsating flow in a rod bundle channel. Exp Thermal Fluid Sci 113:110047

Qu J, Sun Q, Wang H, Zhang D, Yuan J (2019) Performance characteristics of flat-plate oscillating heat pipe with porous metal-foam wicks. Int J Heat Mass Transf 137:20–30

Qu W and Yang B (2009) Performances of flat plate pulsating heat pipes. In: Proceedings of the ASME 2009 second international conference on micro/nanoscale heat and mass transfer, vol 3. ASME, Shanghai, China, pp 403–410

Sagar KR, Naik H, Mehta B (2022) Novel condenser based cryogenic pulsating heat pipe: investigations on influence of geometrical parameters. Cryogenics 126:103543

Shafii MB, Faghri A, Zhang Y (2001) Thermal modeling of unlooped and looped pulsating heat pipes. J Heat Transfer 123(6):1159–1172

Sivasankaran S, Narrein K (2020) Influence of geometry and magnetic field on convective flow of nanofluids in trapezoidal microchannel heat sink. Iran J Sci Technol Trans Mech Eng 44(2):373–382

Srikrishna P, Siddharth N, Reddy S, Narasimham G (2019) Experimental investigation of flat plate closed loop pulsating heat pipe. Heat Mass Transf 55:1–13

Stevens KA, Smith SM, Taft BS (2019) Variation in oscillating heat pipe performance. Appl Therm Eng 149:987–995

Sun Z, Fan R, Zheng N (2021) Thermal management of a simulated battery with the compound use of phase change material and fins: experimental and numerical investigations. Int J Therm Sci 165:106945

Taghilou M, Safavi SA, Khodaei ME (2022) Investigating the effect of heat transfer coefficient and the heat flux on the thermal performance of the pcm in the heat sink. Iran J Sci Technol Trans Mech Eng 46:761–770

Takawale A, Abraham S, Sielaff A, Mahapatra PS, Pattamatta A, Stephan P (2018) A comparative study of flow regimes and thermal performance between flat plate pulsating heat pipe and capillary tube pulsating heat pipe. Appl Therm Eng 149:1359–4311

Thompson SM, Lu H, Ma H (2014) Thermal spreading with flat-plate oscillating heat pipes. J Thermophys Heat Transf 29(2):338–345

Thompson S, Ma H (2010) Effect of localized heating on three-dimensional flat-plate oscillating heat pipe. Adv Mech Eng 2:1–10

Wang Y, Cen J, Jiang F, Cao W (2017) Heat dissipation of high-power light emitting diode chip on board by a novel flat plate heat pipe. Appl Therm Eng 123:19–28

Wits WW, Groeneveld G, Van Gerner HJ (2019) Experimental investigation of a flat-plate closed-loop pulsating heat pipe. J Heat Transf 141(9):091807

Xie XL, Tao WQ, He YL (2007) Numerical study of turbulent heat transfer and pressure drop characteristics in a water-cooled minichannel heat sink. J Electron Packag 129(3):247–255

Xu R, Chen H, Wu Q, Xu S, Wang R (2019) Testing and modeling of the dynamic response characteristics of pulsating heat pipes during the start-up process. J Therm Sci 28(1):72–81

Yang H, Khandekar S and Groll M (2004) Operational characteristics of flat plate closed loop pulsating heat pipes. In: 13th international heat pipe conference, Shanghai, pp 291–297: Shanghai, China

Yoon A, Kim SJ (2017) Characteristics of oscillating flow in a micro pulsating heat pipe: fundamental-mode oscillation. Int J Heat Mass Transf 109:242–253

Yoon A, Kim SJ (2019) Experimental and theoretical studies on oscillation frequencies of liquid slugs in micro pulsating heat pipes. Energy Convers Manage 181:48–58

Zhang D, He Z, Jiang E, Shen C, Zhou J (2021) A review on start-up characteristics of the pulsating heat pipe. Heat Mass Transf 57(5):723–735

Zhang F, Winholtz R, Black W, Wilson M, Taub H, Ma H (2016) Effect of hydrophilic nanostructured cupric oxide surfaces on the heat transport capability of a flat-plate oscillating heat pipe. J Heat Transf 138(6):062901–062907

Springer Nature or its licensor (e.g. a society or other partner) holds exclusive rights to this article under a publishing agreement with the author(s) or other rightsholder(s); author self-archiving of the accepted manuscript version of this article is solely governed by the terms of such publishing agreement and applicable law.